Geotechnical Safety and Risk V
T. Schweckendiek et al. (Eds.)

doi:10.3233/978-1-61499-580-7-281

Stability Analysis of Unsaturated Soil Slope Considering the Variability of Soil-water Characteristic Curve

L. ZHANG and W. M. YAN
Department of Civil Engineering, The University of Hong Kong, Hong Kong, China

Abstract. Soil slopes are generally unsaturated in which the soil-water characteristic curve (SWCC) plays an important role in its hydro-mechanical response. The commonly used Mohr-Coulomb failure criterion in saturated soil mechanics could be extended to take SWCC into account which is then able to determine the shear strength of unsaturated soil. Like many other soil properties, spatial variation of SWCC within a soil domain is expected. It therefore gives a spectrum of varying shear strength across the unsaturated soil slope. In this study, the effect of this spatial variability on slope stability will be investigated. As a first trial, the true cohesion, friction angle and degree of saturation of the unsaturated ground are assumed to be deterministic. SWCC of the soil is described by the van Genuchten model parameters, which are assumed to follow a prescribed probability density function. Therefore, a random field of apparent cohesion due to unsaturation can then be generated using the Cholesky decomposition method. The necessary statistical information for the random fields could be obtained by the Monte Carlo approach based the varied SWCC. The slope stability analysis is carried out using the finite element analysis method. For a given saturation degree, thousands of realizations of the random fields will be generated and the probability of failure is then evaluated. The relationship between the degree of saturation and probability of failure will be examined. Besides, the influence of correlation length of soil shear strength on the probability of failure will also be analyzed.

Keywords. Uncertainty, random field, slope stability, spatial variability, SWCC

1. Introduction

Landslide is a common geohazard and the stability of slopes remains a challenging topic. Numerical techniques such as the finite element method (FEM) offer alternate approach to investigate the slope stability as compared to the classical limit equilibrium method (Griffiths and Lane, 1999). Utilizing probabilistic techniques such as the *First Order Second Moment* (FOSM) or *Point Estimate Method* (PEM), and with an appropriate quantification of the variability of the soil properties, a probabilistic indicator like the *Reliability Index* (RI) or *Probability of Failure* (POF) can be derived to shed light on the stability of the studied slope. Proposed by Griffiths and Fenton (1993), the *Random Finite Element Method* (RFEM) has shown its potential in the stochastic slope stability analysis.

Soil slopes are generally unsaturated in the natural environment. The soil-water characteristics curve (SWCC) which describes the water retention properties of the soil presents an important behavior of the material in its unsaturated state. Fredlund et al. (1978) proposed an extended Mohr-Coulomb failure criterion which takes soil suction into account when evaluating the soil shear strength. Based on Bayesian probabilistic framework, Chiu et al. (2012) analyzed the uncertainty of SWCC. The joint-probability density function (PDF) of the two parameters van Genuchten model (van Genuchten, 1980) was studied and the confidence interval (CI) of SWCC of three different soil types (different soil texture) were given. The CI also indicates the PDF of suction for a given saturation degree of the soil. By incorporating the distribution of suction into the extended Mohr-Coulomb failure criterion, a distribution of apparent cohesion, and thus the soil shear strength, can be obtained.

This study combines the uncertainty of SWCC and the spatial variability of shear strength in a RFEM analysis. The main objective is to investigate the influence of the variability of SWCC on slope stability.

2. Methodology

2.1. RFEM

RFEM considers the random field theory (Thomson, 1983) in a finite element analysis. It allows the spatial variability of soil properties to be considered in the analysis. Gaussian random field is the most widely used random field in which three parameters are required. The magnitude of a soil property φ at a point is described by its mean value μ_φ and standard deviation σ_φ. Correlation length (also called the scale of fluctuation) θ represents the distance over which φ correlates significantly. In this paper, an exponentially decaying correlation function is adopted which is expressed in Eq. (1) for a two-dimensional space.

$$\rho_{ij} = \exp\left[\frac{-2\sqrt{\Delta x_{ij}^2 + \Delta y_{ij}^2}}{\theta}\right] \tag{1}$$

where Δx_{ij} and Δy_{ij} represent the relative distance in the two directions and ρ_{ij} is the correlation coefficient. Higher value suggests higher correlation between the two points.

The Cholesky decomposition method is adopted in this study to generate the random field. Eq. (2) shows the decomposition process. $\boldsymbol{\rho}$ is the covariance matrix with element ρ_{ij}. $\mathbf{L}$ and $\mathbf{L}^\mathrm{T}$ are the lower triangular matrix and its transpose.

$$\boldsymbol{\rho} = \mathbf{L}\mathbf{L}^\mathrm{T} \tag{2}$$

The Gaussian random field can be generated according Eq. (3).

$$\mathbf{R} = \mathbf{L}\mathbf{U} \tag{3}$$

where $\mathbf{U}$ is a column vector which elements are independent Gaussian random numbers with zero mean and unit standard deviation. $\mathbf{R}$ is the generated standard Gaussian random field with the given correlation length. The desired random field $\boldsymbol{\varphi}$ can be calculated by Eq. (4).

$$\boldsymbol{\varphi} = \mu_\varphi \mathbf{I} + \sigma_\varphi \mathbf{R} \tag{4}$$

where $\mathbf{I}$ is a unit column vector.

When mapping the random field to the problem domain, the point statistics have to be transformed through spatial averaging over the element size. For Gaussian random filed, the mean value is unaffected and the standard deviation is scaled as given by Eq. (5).

$$\gamma = \left(\frac{\sigma_A}{\sigma_\varphi}\right)^2 \tag{5}$$

where σ_A is the standard deviation of the spatial averaged value over element size and γ is the variance reduction factor. It is calculated by integrating the correlation coefficient (Eq. (1)) over the element domain. For the two-dimensional square elements used in this paper, γ can be obtained by Eq. (6). Table 1 shows the values of reduction factor for $l = 0.75$ m given different θ given l is the element size.

$$\gamma = \frac{4}{l}\int_0^l\int_0^l \exp\left[\frac{-2}{\theta}\sqrt{x^2+y^2}\right](l-x)(l-y)\mathrm{d}x\mathrm{d}y \tag{6}$$

Table 1. Effect of θ on γ

θ (m)	γ	θ (m)	γ
0.05	0.006	10	0.925
0.1	0.023	20	0.962
1	0.489	30	0.974
2	0.688	50	0.985
5	0.858	100	0.992

Since the variability of soil properties are more likely to have lognormal distribution rather than Gaussian distribution, lognormal random field is used in this paper. The transformation from Gaussian random field to lognormal random field can be easily obtained by considering the statistical fact that if variable x has normal distribution as represented by $\mathrm{N}(\mu,\sigma)$, $\exp[x]$ has lognormal distribution denoted by $\mathrm{LN}(\mu,\sigma)$.

2.2. Uncertainty of SWCC

The van Genuchten model (van Genuchten, 1980) is used in this study to describe a SWCC (Eq. (7)):

$$S = \frac{\theta_w - \theta_r}{\theta_s - \theta_r} = \frac{1}{\left[1+(\alpha \cdot \psi)^n\right]^m} \tag{7}$$

where S, ranging between 0 and 1, is the normalized volumetric water content; θ_w, θ_s, and θ_r are the current volumetric, saturated, and residual water content of the soil respectively; α, n, and m are non-negative fitting parameters; ψ is the matric suction. Following Chiu et al. (2012), $m=1$ is adopted for simplicity. The volumetric water content can be expressed in terms of the degree of saturation S_r and void ratio e as shown in Eq. (8):

$$\theta_w = \frac{eS_r}{1+e} \tag{8}$$

Following Lu and Griffiths (2004), the extended Mohr-Coulomb failure criterion can be written as

$$\tau_f = c' + \left[(\sigma - u_a) + \psi S\right]\tan\phi' \tag{9}$$

where τ_f, σ, and u_a are the shear strength, total normal stress and pore air pressure respectively; c' and ϕ' are the true cohesion and drained friction angle of the soil. A term called apparent cohesion c^a is defined as follows:

$$c^a = \psi S \tan\phi' \tag{10}$$

Due to the variability and uncertainty of SWCC, c^a is not a deterministic value for a given S_r. Chiu et al. (2012) presented the uncertainty of S for three different types of soils based on the UNSODA database, as characterized by Eq. (11):

$$S = \Phi\left[\Phi^{-1}\left(\frac{1}{1+(\alpha\cdot\psi)^n}\right)+\varepsilon\right] \tag{11}$$

where $\Phi[-\infty,+\infty]=[0,1]$ is the cumulative distribution function; the joint-PDF of α and n is evaluated from the data; and ε is assumed to follow a Gaussian distribution with zero mean and standard derivation $\hat{\sigma}_\varepsilon$ in which $\hat{\sigma}_\varepsilon^{\,2}$ is the minimum value of the goodness-of-fit function. In this study, ϕ', θ_s, θ_r and e are assumed as constants (Table 2) while the joint-PDF of α, n and $\hat{\sigma}_\varepsilon$ are assumed to follow the sandy loam soil data given in Chiu et al. (2012). For a given S_r, re-writing Eq. (11) gives

$$\psi = \left[\alpha\cdot\Phi\left(\Phi^{-1}\left(\frac{\frac{eS_r}{1+e}-\theta_r}{\theta_s-\theta_r}\right)-\varepsilon\right)\right]^{-\frac{1}{n}} \tag{12}$$

Table 2. Parameters for the calculation of apparent cohesion

θ_r	θ_s	e	$\hat{\alpha}$	σ_a	$\hat{n}$	σ_n	ϕ'	$\hat{\sigma}_\varepsilon$
0.112	0.388	0.7	0.115	0.008	0.970	0.049	25	0.769

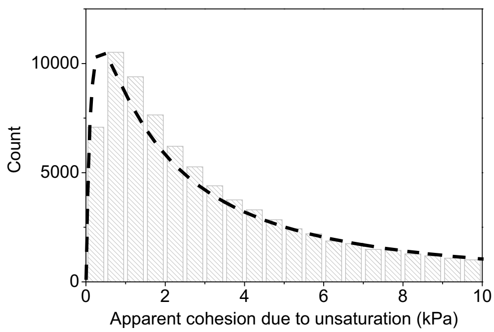

Figure 1. Histogram of apparent cohesions at S_r =40% .

Monte Carlo simulation can then be performed to give ψ and thus c^a according to Eqs. (12) and (10), respectively. In this study, for each S_r, 100,000 samples of c^a are generated. Figure 1 shows the statistical histogram of the generated c^a samples. In each case, a lognormal distribution is proposed for c^a and its statistical information is summarized in Table 3.

Table 3. Fitting parameters for different S_r

S_r	28%	35%	40%	50%
$\mu(c^a)$	1.804	1.505	1.349	1.070
$\sigma(c^a)$	1.832	1.644	1.512	1.414
$\mathrm{CV}(c^a)$	1.016	1.092	1.121	1.321

2.3. FEM Model Configurations

The finite element package ABAQUS is used in this paper to conduct the RFEM. The geometric dimensions as well as the boundary conditions of the slope model are shown in Figure 2. The boundary conditions are given as vertical rollers on the left and right boundaries and full fixity at the bottom boundary.

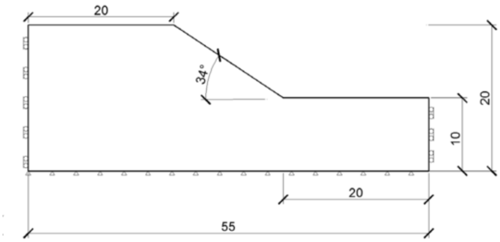

Figure 2. Geometric dimensions of slope model (unit: m).

Linear-elastic perfectly-plastic model with the extended Mohr-Coulomb failure criterion is adopted in the analyses. Table 4 summarizes the model parameters. The true cohesion c^0 and the dilation angle ψ of sandy loam soil are ignored and set to be zero in this paper.

Table 4. Model parameters used in simulation

E (MPa)	μ	ρ (kg/m^3)	c^0 kPa	ϕ (°)	ψ (°)
100	0.3	2000	0	25	0

By considering the lognormal random field generated based on the parameters in Table 3 and a specific correlation length θ, each element in slope model was assigned with different c^a and thus has different shear strengths. As an example, Figure 3 shows the generated random field of c^a given $S_r = 40\%$ and $\theta = 10$ m. The model consisted 1,772 elements. The same mesh configuration was adopted by all the simulations in this paper. Color intensity of an element reveals the magnitude of c^a. The darker the color, the higher c^a it represents. In this case, the ground has a mean c^a of 11.09 kPa.

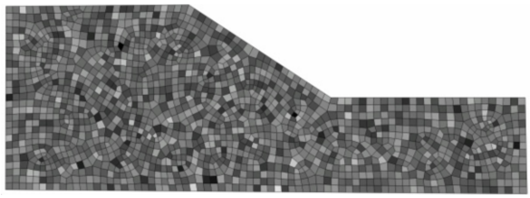

Figure 3. Random field of c^a at S_r = 40% and θ =10 m.

One thousand realizations were generated for each condition. The numerical simulations of some realizations failed as they did not reach convergence, which is defined as failure in this paper. The probability of failure (POF), which is defined as the percentage of failed realizations over the total realizations, is then computed to indicate the stability of the model slope.

3. Results and Discussion

3.1. Influence of the Number of Realizations

In order to obtain a converging result of POF, sufficient realizations are required. The evolution of POF with realizations, given $S_r = 40\%$ and $\theta = 10$ m, is shown in Figure 4. It indicates that as the number of realizations increases, the POF converges to an essentially constant value. The figure shows that 1,000 realizations are sufficient for POF calculation in this paper.

3.2. Influence of the Correlation Length

Figure 5 shows the evolutions of POF with increasing correlation lengths for different saturation degrees. Two different types of evolutions of POF for the four selected S_r can be seen. For S_r = 28, 35 and 40%, POF firstly increases and then gives a steady value with a further increase in the correlation length. On the contrary, POF first decreases before reaching a steady value at larger correlation length for $S_r = 50\%$. At a very small correlation length, for instance $\theta = 0.1$ m, POF is small (very low chances of failure) when S_r is small but becomes large (close to unity, i.e., very high chances of failure) when S_r becomes large.

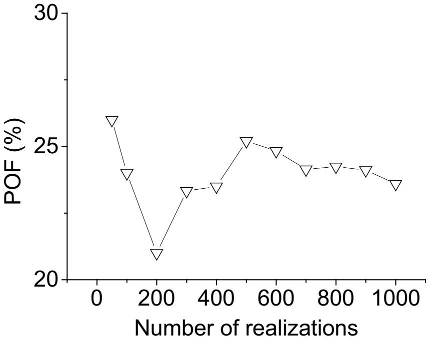

Figure 4. Evolution of POF with the number of realizations.

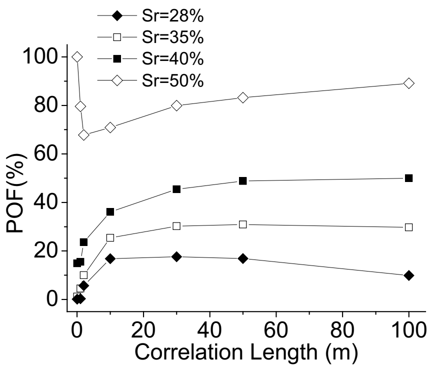

Figure 5. POF versus correlation length

Similar phenomenon was also observed in Griffiths and Fenton (2004). Recalling the variation reduction effect of the correlation length shown in Table 1, smaller correlation length corresponds to a more homogenous ground. Therefore, the variation of slope model is expected to be small and the result of finite element analysis across different realizations tends to be very similar. For low S_r and small θ, therefore, any realization should be rather homogenous and has relatively high shear strength. A low POF is expected. When θ becomes larger, the variations of shear strength in any slope model become higher. In other words, the chances of having soil with lower shear strength become higher, and therefore POF increases. By the same token, the trend of decreasing POF with increasing θ for high S_r could also be explained.

4. Conclusion

The random field theory and uncertainty of SWCC are reviewed. Slope stability analysis with RFEM based on lognormal random field was implemented in ABAQUS and several conclusions were obtained. First, the distribution of apparent cohesion by considering the uncertainty of SWCC could be well described with lognormal distribution. Second, the evolution of POF with increasing number of realizations was analyzed and 1,000 realizations were proved to be sufficient in this study. Third, the POF changes rapidly with increasing correlation length. For each degree of saturation, POF converges to a steady value when the correlation length becomes higher.

Acknowledgement

The authors would like to acknowledge the research grant HKUST6/CRF/12R provided by the Research Grants Council of the Hong Kong Special Administrative Region (HKSAR).

References

Chiu, C.F., Yan, W.M., Yuen, K.-V. (2012). Reliability analysis of soil–water characteristics curve and its application to slope stability analysis. *Engineering Geology* **135**, 83-91.

Fredlund, D.G., Morgenstern, N., Widger, R. (1978). The shear strength of unsaturated soils. *Canadian Geotechnical Journal* **15**(3), 313-321.

Fredlund, D.G., Xing, A., Fredlund, M.D., Barbour, S. (1996). The relationship of the unsaturated soil shear to the soil-water characteristic curve. *Canadian Geotechnical Journal* **33**(3), 440-448.

Griffiths, D.V., Fenton, G.A. (2004). Probabilistic slope stability analysis by finite elements. *Journal of Geotechnical and Geoenvironmental Engineering* **130**(5), 507-518.

Griffiths, D.V., Lane, P. (1999). Slope stability analysis by finite elements. *Géotechnique* **49**(3), 387-403.

Griffiths, D.V., Fenton, G.A. (1993). Seepage beneath water retaining structures founded on spatially random oil. *Géotechnique* **43**(4), 577-587.

Lu, N., Griffiths, D.V. (2004). Profiles of steady-state suction stress in unsaturated soils. *Journal of Geotechnical and Geoenvironmental Engineering* **130**(10), 1063-1076.

Thomson, D.J. (1983). Random Fields: Analysis and Synthesis. *Eos, Transactions American Geophysical Union* **64**(37), 550-550.

van Genuchten, M.Th. (1980). A closed-form equation for predicting the hydraulic conductivity of unsaturated soils. *Soil Science Society of America Journal* **44**(5), 892-898.